PMSM Drive Position Estimation: Contribution to the High-Frequency Injection Voltage Selection Issue

Slimane Medjmadj, Demba Diallo, *Senior Member, IEEE*, Mohammed Mostefai, Claude Delpha, *Member, IEEE*, and Antoni Arias, *Member, IEEE*

***Abstract*—High-frequency injection (HFI) is an alternative method to estimate permanent magnet synchronous motor (PMSM) rotor position using magnetic saliency. Once the maximum fundamental electrical frequency and the power converter switching frequency are set, the HFI voltage amplitude tuning is generally based on trial and error. This paper proposes a methodology to select the appropriate high-frequency signal injection voltage amplitude for rotor position estimation. The technique is based on an analytical model taking into account the noise in the voltage supply to derive the resulting currents containing the information on the rotor position. This model allows setting the injection voltage amplitude that leads to the maximum acceptable position error for a given signal-to-noise ratio and a speed range. The approach is validated with the analytical and the global drive models through extensive simulations. Experimental results on a 1-kW PMSM drive confirm the interest of the proposed solution.**

***Index Terms*—AC motor drives, Gaussian noise, permanent magnet synchronous motor (PMSM), rotor position estimation, signal-to-noise ratio (SNR).**

NOMENCLATURE

$\theta_r, \hat{\theta}_r$	Actual and estimated rotor electric position (rad)
θ	Rotor mechanical position (rad).
L_d, L_q	*d* and *q*-axis stator inductances, respectively (H).
R_s	Stator resistance (Ω).
$V_\mathrm{a}, V_\mathrm{b}, V_\mathrm{c}$	Voltages in the (*a,b,c*) reference frame (V).
$V_\alpha, V_\beta, i_\alpha, i_\beta$	Voltages and currents in the Clark (α,β) reference frame.
V_d, V_q, i_d, i_q	Voltages and currents in the Park (*d,q*) reference frame.
ψ_α, ψ_β	Fluxes in (α,β) frame (Wb).
ψ_d, ψ_q	Fluxes in (*d,q*) frame (Wb).
ψ_m	Rotor flux due to the permanent magnets (Wb)
w_r	Electrical rotor speed (rad/s).
$\Omega, \hat{\Omega}$	Actual and estimated rotor speed (rad/s).
Ω_ref	Rotor speed reference (rad/s).
ρ	Derivative operator *d/dt.*
f_i	Injection frequency (Hz), (rad/s), $\omega_i = 2\pi f_i$
V_{si}	High-frequency-injected carrier voltage (V).
V_m	Maximum voltage amplitude (V).
n_1, n_2, n_3	Additive noise amplitudes in (*a,b,c*) reference frame (V).
SNR	Signal-to-noise ratio (dB).
AWGN	Additive white Gaussian Noise.
σ^2	Variance
μ	Mean value.
PSD	Power spectral density.
$\varepsilon_\theta = \theta_r - \hat{\theta}_r$	Rotor position error (rad).
ε_{AM}	Rotor position error of the analytical model (rad).
ε_{GM}	Rotor position error of the global model (rad).

Manuscript received March 18, 2014; revised June 30, 2014; accepted July 30, 2014. Paper no. TEC-00204-2014.

S. Medjmadj is with the Laboratory of Control (LAS), University Bordj Bou Arreridj, Bordj Bou Arréridj 34000, Algeria (e-mail: s_medjmadj@yahoo.fr).

D. Diallo is with the Laboratoire de Génie Electrique de Paris, French National Centre of Research (CNRS), Supélec, Univ. Paris Sud, Univ. Pierre et Marie Gurie, 91192 Gif Sur Yvette, 75005 Paris, France (e-mail: ddiallo@ieee.org).

M. Mostefai is with the Laboratory of Control (LAS), Department of Electrical Engineering, Faculty of Technology, University Ferhat Abbas Setif, Setif 19000, Algeria (e-mail: mostefai@univ-setif.dz).

C. Delpha is with the Laboratoire des Signaux et Systémes, French National Centre of Research (CNRS), Supélec, Univ. Paris Sud, 91192 Gif Sur Yvette (e-mail: claude.delpha@u-psud.fr).

A. Arias is with the University Politecnica de Catalyuna, 08034 Barcelona, Spain (e-mail: antoni.arias@upc.edu).

Color versions of one or more of the figures in this paper are available online at http://ieeexplore.ieee.org.

Digital Object Identifier 10.1109/TEC.2014.2354075

I. INTRODUCTION

PERMANENT magnet synchronous motors (PMSMs) have good performances, such as high-energy density, fast dynamic response, and good overload capacity. They are widely used in a variety of industrial applications, such as industrial robots, aeronautics, electric vehicle, and machine tools [1]–[4]. In order to achieve high precision and fast dynamic control characteristics of PMSMs, an accurate rotor position measurement is necessary. This is usually done with a mechanical sensor, which will not only bring a cost increment but more importantly it might raise reliability issues due to the fact that such sensors are delicate and need additional electronics as well as extra cabling. Moreover, sensorless algorithms, even when using position sensors, are useful in case of any failures, as it may be used as a redundant sensor and, therefore, a fault tolerant control can be achieved. Therefore, there has been a high research activity focused on eliminating the position sensors mounted on the rotor of the PMSM machines to obtain the rotor position information indirectly [5]–[7].

In general there are three strategies. The first one is the knowledge-based (such as artificial intelligence, genetic algorithms, fuzzy logic, etc.) [8]–[10]. These methods suffer from the need of data recorded on the process to train the networks. The second one is physical-model-based approach, such as

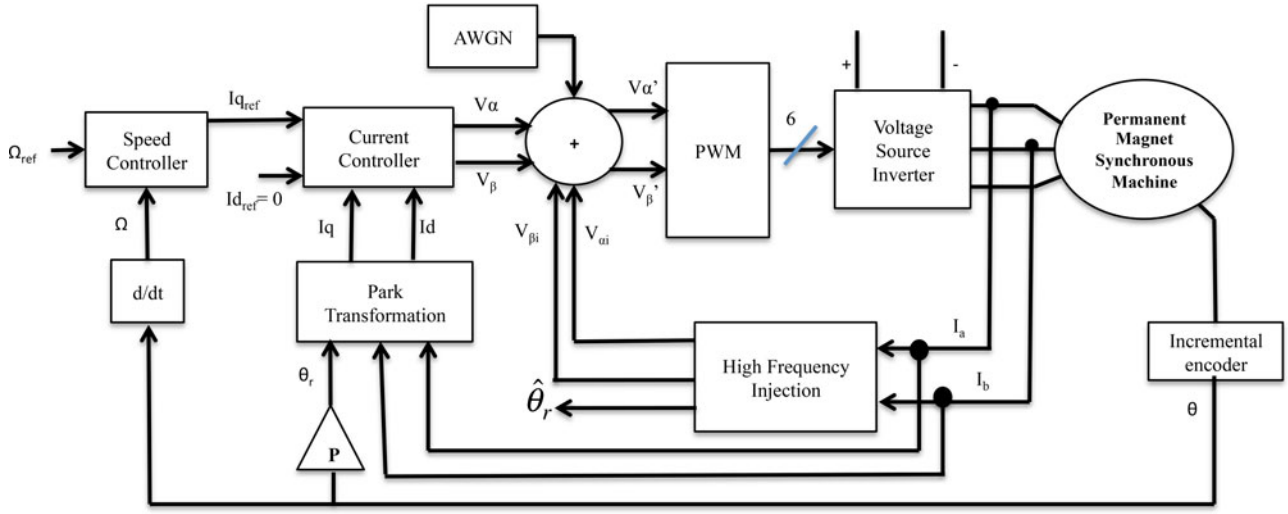

Fig. 1. PMSM drive with HF voltage injection and noise addition.

observers and estimators (MRAS, Luenberger, Extended Kalman Filter, Sliding Mode Observer, Differential Algebraic, etc.) [11]–[13].

These methods are mostly efficient for high speeds and have the disadvantages of heavy computation, especially when facing nonsuboptimal Kalman Filters. They mainly suffer from the modeling errors or assumptions. For these reasons, significant research efforts have been conducted to develop alternative methods, such as high-frequency (HF) signal injection [14] as displayed in Fig. 1.

Even if it requires a PMSM with magnetic saliency, this approach seems promising particularly at low speed where the other methods usually fail

II. High Frequency Injection (HFI) and Problem Statement

A. HFI Principle

The technique consists in injecting either a pulse or a sinusoidal test signal in order to be able to track the existing magnetic saliency without introducing torque ripples.

The main issues are on the selection of the pulse shape, the frequency, and the voltage amplitude. In the following, we focus on sinusoidal excitation. On one hand, the frequency is usually set in a range ten times higher than the maximum fundamental frequency and ten times lower than the power converter switching frequency. On the other hand, the voltage amplitude selection is somehow a random process. Too low-voltage amplitude will not generate enough current, and if the amplitude is too high, undesirable torque ripples will appear.

The injection of a rotating HF voltage for saliency tracking has been proposed by several authors [15]–[17]. Several methods using analog filters and frequency shifts may be used to isolate the rotor position information. In [18], it is shown that the rotor position estimator for salient-pole PMSM is given by using only one low-pass filter (LPF). In our study, the position estimation is derived from a HF current injection by using three

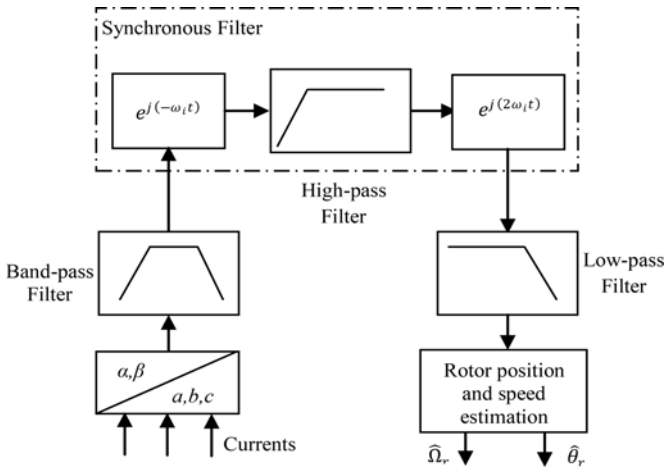

Fig. 2. Synchronous filters for demodulation of HF currents.

filters: A LPF, a high-pass filter (HPF), and a band-pass filter (BPF), and the position estimation bias is cancelled thanks to a phase compensation scheme. A brief review of this process is displayed in Fig. 2 and [19]–[22].

B. Noise Effect Analysis and Paper's Contribution

Usually, the HFI voltage amplitude is set by trial and tuned so as to have accurate position estimation after the demodulation. Our approach consists in determining with a theoretical approach how to set the minimum value of the HFI voltage amplitude that still guarantees good position estimation despite the noise level due to the inverter and the application environment.

This is done through an analytical model that will be presented in this paper. And to evaluate the noise effect with this theoretical approach, the AWGN is the most popular and usual noise model as it consists in adding a noise with a constant power all over the spectrum without emphasizing any particular frequency.

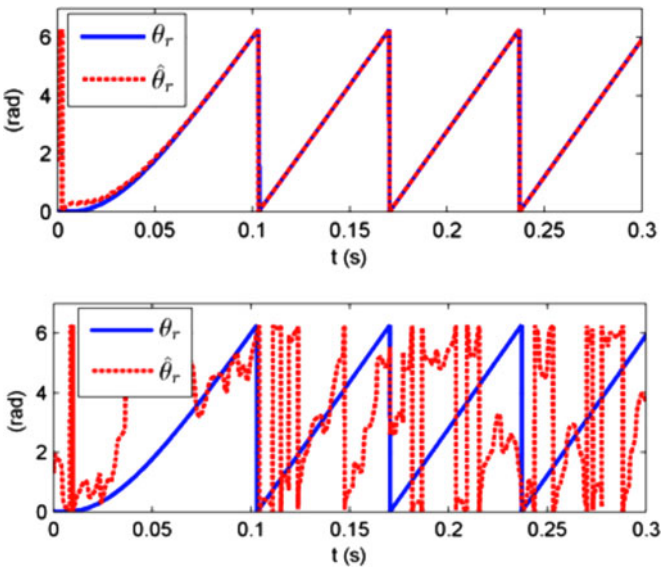

Fig. 3. Actual and estimated rotor positions with the global model (in electrical radian).

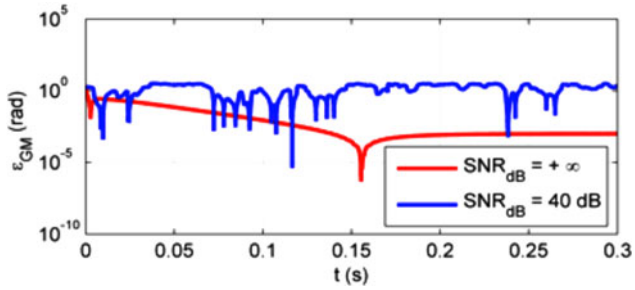

Fig. 4. Rotor position errors with the global model (in electrical radian).

In the following, global model is denoted as the model including the PMSM, the field oriented control, the load, the HFI, and demodulation modules and the AWGN as displayed in Fig. 1.

It will be used as the reference to evaluate the analytical model developed in the following section. The environment is noisy due to the inverter switching and all the other perturbations [23]–[25]. This can be taken into account by considering SNR ($\mathrm{SNR_{dB}}$) defined as

$$\mathrm{SNR_{dB}} = 10\log_{10}\left(\frac{\sigma^2_{\mathrm{signal}}}{\sigma^2_{\mathrm{noise}}}\right) \tag{1}$$

where σ^2 is the variance. Both signal and noise power must be measured at the same or/and equivalent points in a system, and within the same system bandwidth.

To illustrate the noise effect on the studied system, a simulation of the PMSM drive has been done with an estimator based on HFI. The comparison is made between an ideal case with a very high $\mathrm{SNR_{dB}}$; meaning there is no noise [see Fig. 3(a)] and a noisy environment with an $\mathrm{SNR_{dB}}$ of 40 dB [see Fig. 3(b)], a usual value in electrical systems.

Fig. 3 displays the actual and estimated rotor position. Fig. 4 shows the absolute value of the estimated rotor position error. We can clearly see the negative influence of the noise in the estimation performance. Of course increasing the voltage amplitude will improve the result but to what extent?

On the other hand, the injection voltage value should be kept to a minimum because it introduces additional losses. However, a very small, and therefore ideal, injection value would threaten the quality of the estimation due to the noise, as it has been pointed before. Therefore, a clear compromise exists in setting such value. Traditionally, such compromise has been solved with a trial and error process at the experimental stage. Rather than proposing a variation on, or an improvement of the well-known HFI technique [14]–[20], this paper establishes new criteria to conveniently set the injection voltage amplitude taking into account the noisy environment. Also, the contribution relies on the fact that such voltage amplitude value is discussed in a more analytical approach surpassing the experimental trial an error traditional methodology. The paper is organized as follows. In Section III, the analytical model of the PMSM under HF voltage excitation including the noise is established to derive the resulting injection currents. In Section IV, the model is evaluated through intensive simulations and the results are compared to those obtained with the whole drive simulation. In Section V, we present experimental implementation of this HFI estimator and the comparison with simulation results. Finally, a conclusion is drawn in Section VI.

III. Dynamic Analytical HFI-PMSM Model

For all injection methods to work, a minimum saliency level is needed. Injection techniques are more straightforward for salient machines such as interior PMSM than for surface mount PMSM, which only possess a small saliency due to magnetic saturation caused by the permanent magnet. This makes the technique prone to interference from distorting effects such the converter nonlinearities [23]–[25] in addition to spatial field nonlinearities in the machine [6], [7].

When a HF voltage is applied to the machine windings, the resulting HF current signal contains the rotor position information. By demodulating those currents, the rotor position can therefore be estimated.

The analytical model includes the additional noise to the voltage supply and computes the resulting HF injected currents.

A. Analytical Model of the PMSM With HFI

The stator voltage model in the rotor reference frame for a PMSM is given by

$$\begin{bmatrix} V_d \\ V_q \end{bmatrix} = \begin{bmatrix} R_s & 0 \\ 0 & R_s \end{bmatrix} \begin{bmatrix} i_d \\ i_q \end{bmatrix} + \begin{bmatrix} \rho & -w_r \\ w_r & \rho \end{bmatrix} \begin{bmatrix} \Psi_d \\ \Psi_q \end{bmatrix} \tag{2}$$

where ρ is a differential operator. The magnetic flux is given by

$$\begin{bmatrix} \Psi_d \\ \Psi_q \end{bmatrix} = \begin{bmatrix} L_d & 0 \\ 0 & L_q \end{bmatrix} \begin{bmatrix} i_d \\ i_q \end{bmatrix} + \begin{bmatrix} \psi_m \\ 0 \end{bmatrix}. \tag{3}$$

Transforming (2) into the stationary reference frame ($w_r = 0$) results in the following stator voltage equations:

$$\begin{bmatrix} V_\alpha \\ V_\beta \end{bmatrix} = \begin{bmatrix} R_s & 0 \\ 0 & R_s \end{bmatrix} \begin{bmatrix} i_\alpha \\ i_\beta \end{bmatrix} + \begin{bmatrix} w_r & 0 \\ 0 & w_r \end{bmatrix} \begin{bmatrix} \Psi_\alpha \\ \Psi_\beta \end{bmatrix}. \quad (4)$$

The HFI voltages with constant amplitude and angular frequency ω_i are described as follows [5], [21]:

$$\begin{bmatrix} V_{\alpha i} \\ V_{\beta i} \end{bmatrix} = V_{si} \begin{bmatrix} -\sin(\omega_i t) \\ \cos(\omega_i t) \end{bmatrix}. \quad (5)$$

For HF signals, the stator resistance and the effects of the permanent magnet flux linkages can be neglected. A PMSM has a small saliency mainly due to stator saturation from the main magnets.

After applying a BPF centered at the HFI frequency, the following currents are obtained [19], [21], [22]:

$$\begin{bmatrix} I_{i0}\cos(\omega_i t) + I_{i1}\cos(2\theta_r - \omega_i t) \\ I_{i0}\sin(\omega_i t) + I_{i1}\sin(2\theta_r - \omega_i t) \end{bmatrix}$$

$$I_{i0} = \frac{V_{si}(L_q + L_d)}{2w_i L_q L_d}; \quad I_{i1} = \frac{V_{si}(L_q - L_d)}{2w_i L_q L_d}. \quad (6)$$

In order to extract the angle information contained in the negative sequence component I_{i1}, the synchronous filter signal processing steps detailed in Fig. 2 have to be applied. By doing the Park transformation with a rotating frequency equal to minus the injected one ($-\omega_i/2\pi$), the novel currents are

$$\begin{bmatrix} I_{i0} + I_{i1}\cos(2\theta_r - 2\omega_i t) \\ I_{i0} + I_{i1}\sin(2\theta_r - 2\omega_i t) \end{bmatrix}. \quad (7)$$

A HPF is then applied to (8) obtaining

$$\begin{bmatrix} I_{i1}\cos(2\theta_r - 2\omega_i t) \\ I_{i1}\sin(2\theta_r - 2\omega_i t) \end{bmatrix}. \quad (8)$$

To move the angle information back to the fundamental reference frame the Park transform is applied with a rotating frequency equal to ($+2\omega_i/2\pi$), and the information appears as follows:

$$\begin{bmatrix} I_{i1}\cos(2\theta_r) \\ I_{i1}\sin(2\theta_r) \end{bmatrix}. \quad (9)$$

Finally to estimate the electrical angle the arctangent function must be applied

$$2\hat{\theta}_r = \tan^{-1}\left(\frac{I_{i1}\cos(2\theta_r)}{I_{i1}\sin(2\theta_r)}\right). \quad (10)$$

Depending on the quality of the estimation and the overall bandwidth an additional LPFmay be applied, as Fig. 2 illustrates.

B. HFI Model for Position Estimation in Noisy Environment

Now we assume that an AWGN is superimposed to the three phase voltages as follows:

$$\begin{bmatrix} V_{an} \\ V_{bn} \\ V_{cn} \end{bmatrix} = V_{si} \begin{bmatrix} \cos(\omega_i t) \\ \cos\left(\omega_i t - \frac{2\pi}{3}\right) \\ \cos\left(\omega_i t + \frac{2\pi}{3}\right) \end{bmatrix} + \begin{bmatrix} n_1 \\ n_2 \\ n_3 \end{bmatrix} \quad (11)$$

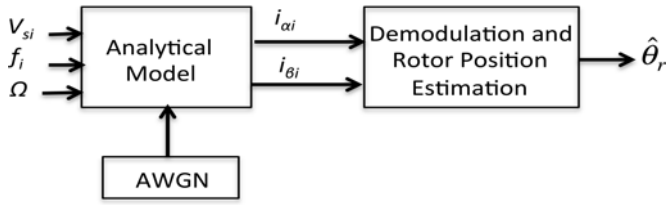

Fig. 5. Estimation of the PMSM rotor position using the analytical model of the HFI in noisy environment.

where $n_1 \neq n_2 \neq n_3$.

After transforming the balanced HF voltage from the *(a,b,c)* frame to the two-phase reference frame we obtain

$$\begin{bmatrix} V_{\alpha\mathrm{in}} \\ V_{\beta\mathrm{in}} \end{bmatrix} = \begin{bmatrix} -V_{si}\sin(\omega_i t) + N_\alpha \\ V_{si}\cos(\omega_i t) + N_\beta \end{bmatrix} \quad (12)$$

where $N_\alpha = \frac{2}{3}n_1 - \frac{n_2}{3} - \frac{n_3}{3}$; $\quad N_\beta = \frac{\sqrt{3}}{3}n_2 - \frac{\sqrt{3}}{3}n_3$.

Combining (6) and (12), the analytical model is derived to compute the resulting derivatives of the currents

$$\begin{cases} \dfrac{di_{\alpha i}}{dt} = -I_{i0}\omega_i\sin(\omega_i t) + I_{i1}\omega_i\sin(2\theta_r - \omega_i t) \\ \qquad +L_1(N_\alpha\cos(2\theta_r) + N_\alpha\sin(2\theta_r)) + L_2 N_\alpha \\ \dfrac{di_{\beta i}}{dt} = I_{i0}\omega_i\cos(\omega_i t) - I_{i1}\omega_i\cos(2\theta_r - \omega_i t) \\ \qquad +L_1(N_\beta\sin(2\theta_r) - N_\beta\cos(2\theta_r)) + L_2 N_\beta \end{cases} \quad (13)$$

where $L_1 = \frac{L_q - L_d}{2L_q L_d}$; $\quad L_2 = \frac{L_q + L_d}{2L_q L_d}$.

In (13), with no noise ($N_\alpha = N_\beta = 0$), one can find the usual model of the HFI and demodulating the currents gives access to the rotor position. In (13), one can also notice that the noise clearly corrupts the rotor position estimation. Fig. 5 shows how the analytical model is used to evaluate the rotor position estimation.

This is confirmed by the results displayed in Fig. 6(b). This analytical model is a useful tool to evaluate the impact of the noise on the rotor position estimation quality.

Fig. 6 displays the actual and estimated rotor position with the analytical model. Fig. 7 shows the absolute value of the estimated rotor position error in semilog scale.

IV. Simulation Results

A. Analytical Model Results

The simulations are performed with MATLAB–Simulink. The parameters of the PMSM are listed in Table I.

The operating point is set in the low-speed region ($\Omega < 10\%\Omega_n$] at no load, where Ω_n is the nominal speed in rad/s.

The HFI signal voltage is set in the range of [0, $10\%V_m$], where $V_m = 12$ V.

Fig. 8 shows the performances of the speed and position tracking obtained with the analytical model when the reference speed is changed from ($+10$ rad/s) to (-10 rad/s).

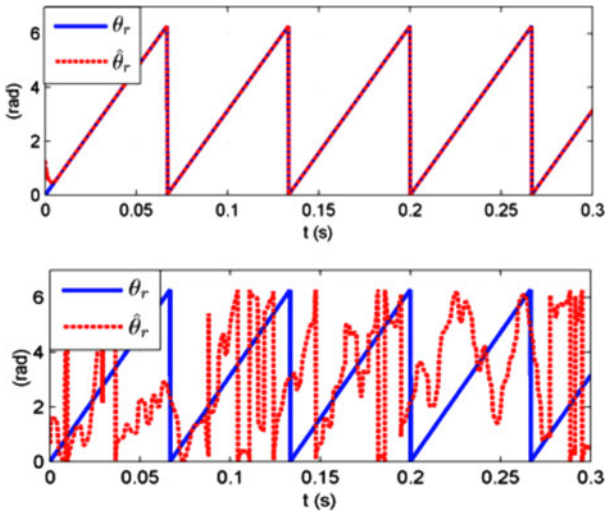

Fig. 6. Actual and estimated rotor position with the analytical model (in electrical radian).

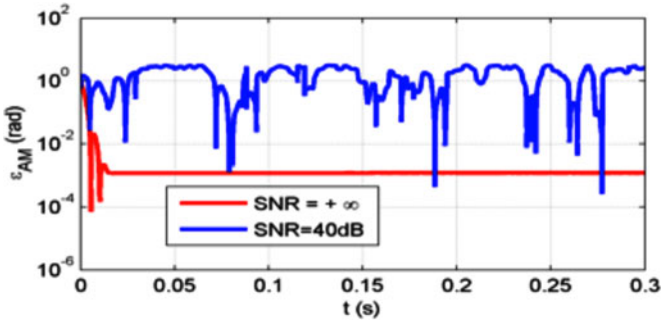

Fig. 7. Rotor position errors with the analytical model (in electrical radian).

TABLE I
SURFACE MOUNT PMSM CHARACTERISTICS

Symbol	Definition	Value
P_n	Nominal power	1.1 kW
Ω_n	Nominal speed	356 rad/s
T_n	Load torque	3.2 Nm
P	Pole pairs	3
In	Nominal current	5.9 A
R_s	Stator resistance	1.65 Ω
L_d	d-axis inductance	3.5 10^{-3} H
L_q	q-axis inductance	4.5 10^{-3} H
Ψ_m	Magnetic flux	154 10^{-3} Wb
f	Viscous friction	509 10^{-3} Nm/rad
J	Moment of inertia	6.4 10^{-3} kg/m^2

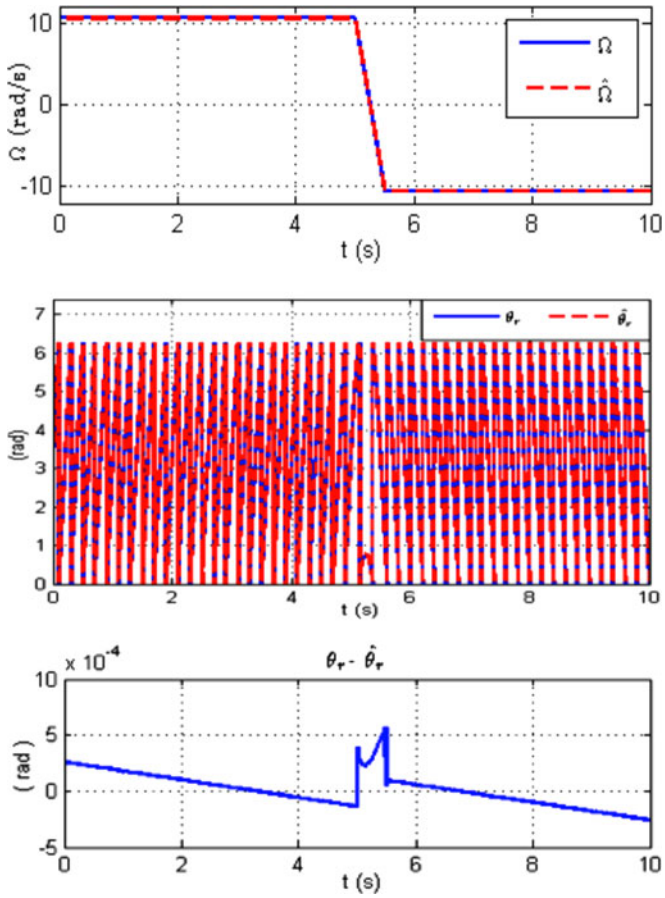

Fig. 8. Simulation results with the analytical model during a speed reversal test.

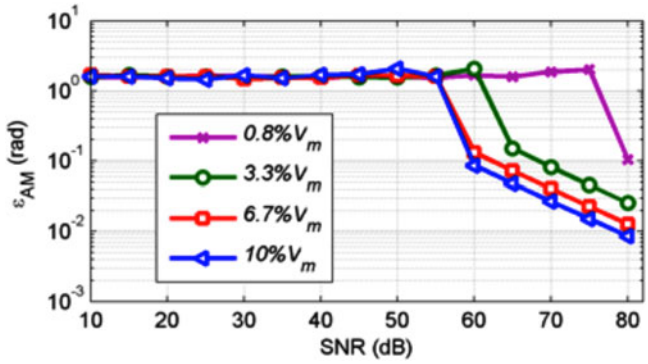

Fig. 9. Effect on the position error signal obtained with the analytical model in noisy environment (in electrical radian).

B. Comparison Between Global and Analytical Models

Figs. 9 and 10 show the influence of the voltage amplitude (expressed as a percentage of V_m) on the position error for different $\mathrm{SNR_{dB}}$ levels with the analytical and the global model respectively.

The error between the actual and the estimated position is computed as follows:

$$\varepsilon_{\mathrm{AM}} = \varepsilon_{\mathrm{GM}} = |\theta_r - \hat{\theta}_r|. \tag{14}$$

Simulation results for both models show that the increase of the injected voltage amplitude in the noisy environment significantly improves the performance of the HFI for the rotor position estimation. The discrepancies of roughly (5 dB) are due to the differences between the two models. Let's recall that the global model includes the speed and current control loops of the PMSM model, while the analytical model is a straightforward relation of the resulting injected currents.

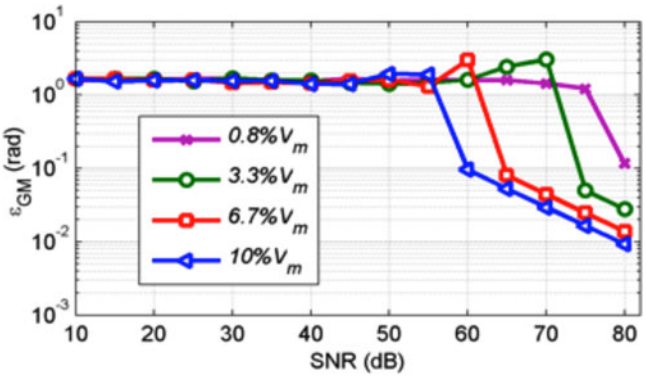

Fig. 10. Effect of on the position error signal obtained with the global model in noisy environment (in electrical radian).

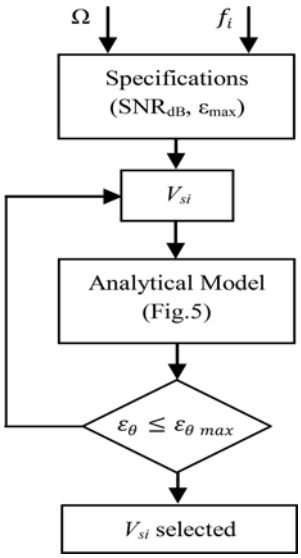

Fig. 11. Flowchart of the injection voltage setting.

For both models, the error decreases significantly from around $\mathrm{SNR_{dB}} = 55$ dB, if the injected voltage amplitude is high enough (6.7% and 10% of V_m). It allows a better estimation of the rotor position. The differences between the two models for high SNR values is due to the numerical effects of the simulation in the global model that includes the vector control and the PMSM model. The main advantage of the analytical model is the short computation time compared to the global model. Therefore, it can be used to evaluate quickly the efficacy of the voltage injection for rotor position estimation. The flowchart depicted in Fig. 11 describes the proposed approach.

For a given speed range and injection frequency, the user specifies the SNR and the maximum acceptable rotor position estimation error (for his application and thanks to the analytical model), the injection voltage amplitude is set appropriately. One way to evaluate the $\mathrm{SNR_{dB}}$ is described in Fig. 12. The LPF and HPF filters are tuned so as to respectively include and reject the injected fundamental frequency (the maximum being 170 Hz

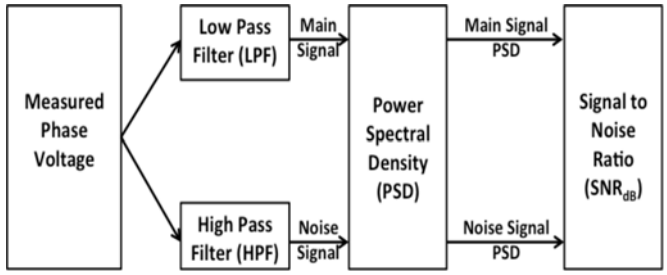

Fig. 12. SNR computation process.

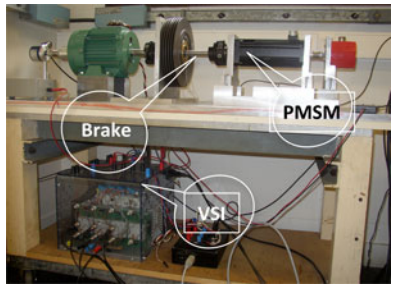

Fig. 13. Laboratory test bed.

in our application). The SNR is computed with (1) after the determination of the PSD.

In Section V, the experimental validation of our approach is presented.

V. Experimental Results

The nominal controller based on the standard vector control and the estimator HFI are implemented on a PMSM drive as displayed in Fig. 13 with the parameters shown in Table I, using MATLAB–Simulink and downloaded in a dSpace 1103 board. The current control algorithm is carried out every 100 μs, and the speed control loop is carried out every 1 ms.

The inverter switching frequency is 20 kHz, and the dc bus voltage is set at 200 V.

The operation point is set at no load with a mechanical speed of 31.4 rad/s (corresponding to 10% of the motor maximal speed).

The amplitude of the HFI voltage is set manually through the graphical user interface of control desk and the measured and estimated rotor position are computed as shown in Fig. 1.

The results are displayed in Fig. 14 with different amplitudes of the voltage. We can notice clearly the improvement of the position estimation as the voltage increases.

For comparison purpose, considering 2 s of time duration, mean values and variances of the estimation errors for the analytical model, the global model, and the experimental drive are displayed in Table II.

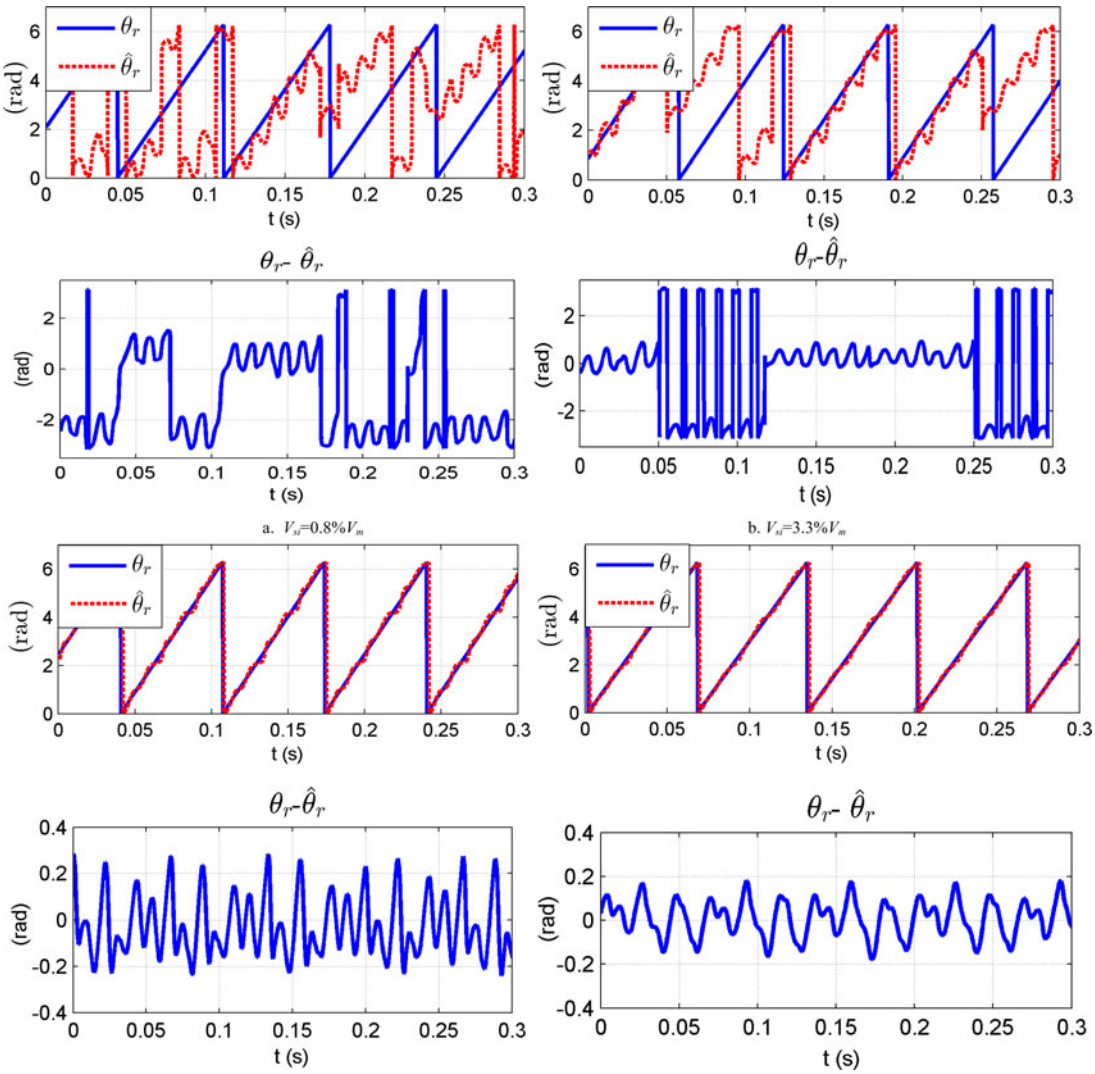

Fig. 14. Actual, estimated and errors rotor position under different voltages levels injection (all angles are in electrical radian). (a). $V_{si} = 0.8\%V_m$. (b). $V_{si} = 3.3\%V_m$. (c). $V_{si} = 6.7\%V_m$. (d). $V_{si} = 10\%V_m$.

TABLE II
CHARACTERISTICS OF THE ESTIMATION ERRORS

V_{si} (%V_m)		0.8	3.3	6.7	10
Analytical model	μ	$14e^{-2}$	$5e^{-2}$	$-1e^{-3}$	$-1e^{-3}$
	σ^2	11.7	8.9	$3e^{-4}$	$3e^{-4}$
Global model	μ	$12e^{-2}$	$-6e^{-2}$	$-15e^{-4}$	$-4e^{-4}$
	σ^2	15	6.25	$6e^{-4}$	$3e^{-5}$
Experiment	μ	$-94e^{-2}$	$-13e^{-2}$	$-7e^{-2}$	$-4e^{-2}$
	σ^2	7.64	5.21	$7.9e^{-4}$	$3.9e^{-4}$

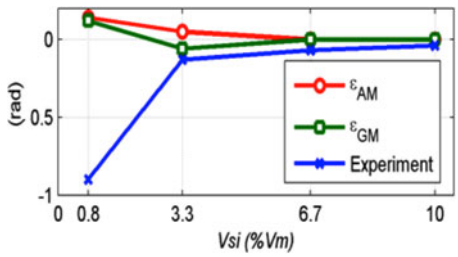

Fig. 15. Mean value of position errors (in electrical radian) for SNR = 62dB.

From these results, we can notice the following.

1) All the values are in the same order of amplitude; therefore, the analytical model is a relevant approach in setting the HFI voltage amplitude.
2) The more the voltage increases; lower are the mean value and the variance of the estimation errors.

Fig. 15 displays the estimation errors mean value. However, one can also notice that the injected voltage (from 6.7 % to10 %) led to an improvement of the estimation at the detriment of higher injected currents and torque ripples. The consequence is the reduction of the efficiency despite a better position estimation accuracy. This is confirmed by the oscillation in the torque current as displayed in Fig. 16.

A summary of its experimental mean values and variances are displayed in Table III.

However, the speed estimation is still accurate with fewer ripples as it can be seen in Fig. 17.

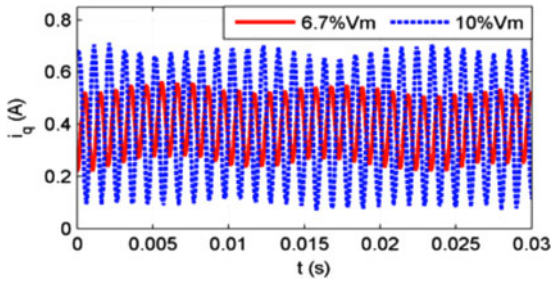

Fig. 16. Stator torque current at 31.4 rad/s.

TABLE III
CHARACTERISTICS OF THE i_q COMPONENT

V_{si} (%V_m)		0.8	3.3	6.7	10
Experiment	μ	0.37	0.37	0.38	0.38
	σ^2	2.8e^{-7}	3.2e^{-6}	1.1e^{-4}	2e^{-3}

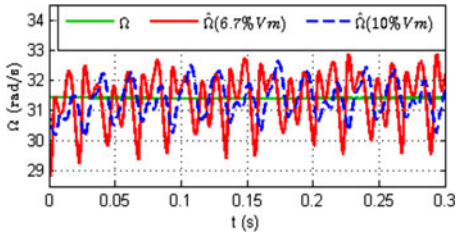

Fig. 17. Measured and estimated speeds.

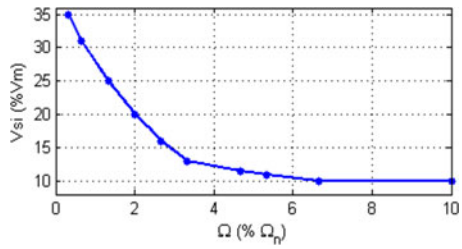

Fig. 18. HFI voltage amplitude.

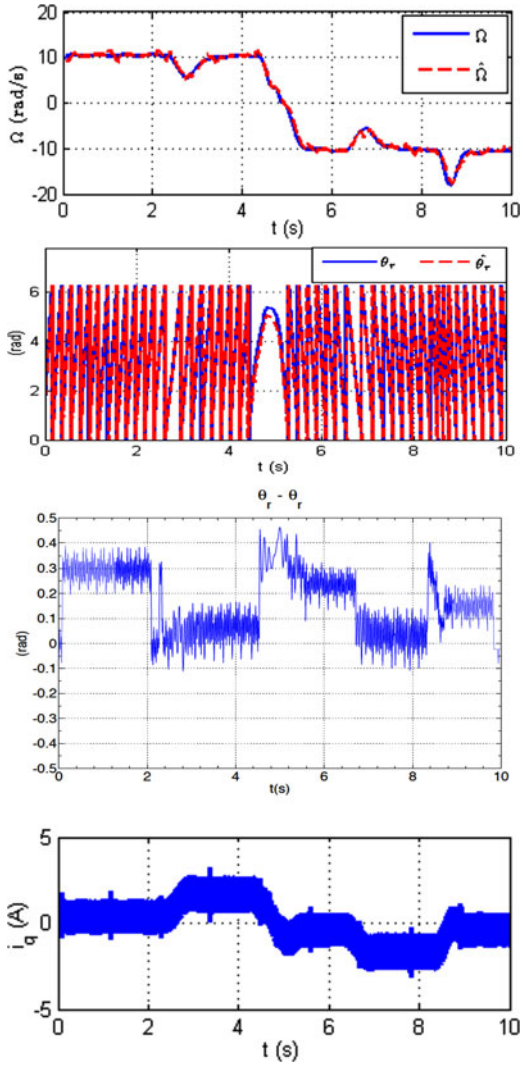

Fig. 19. Experimental results during a speed reversal test under load torque.

Looking at Fig. 18, one can notice that for the same position estimation error, the HFI voltage amplitude can be decreased as the speed increases from 1 (0.33% Ω_n) to 31.4 rad/s (10% Ω_n).

To improve the estimation of the HFI, it is necessary to evaluate the robustness against load torque variations and speed reversal.

Fig. 19 displays the experimental results with a time varying speed reference from $+10$ to -10 rad/s and a step resistive torque of 0.5 Nm (produced by setting the powder brake current) applied in the time ranges [2.3–4.5s] and [6.3–8.3s] is added to the friction torques. These results show the performances of the mechanical rotor speed and rotor electric position tracking capabilities of the HFI. The position error estimation varies in the ± 0.3 electrical radian range (corresponding to ± 0.1 radian for the mechanical angle), which is an acceptable error to further close the loop. However, it must be pointed that the load dependent error, which can be easily compensated for, has not been implemented in the present experimentation. This is why the error changes whenever there is a change of load.

VI. CONCLUSION

In this paper, we have proposed a methodology to set efficiently the voltage amplitude of the HF injected signal in PMSM drive for rotor position estimation. The main contribution is the development of an analytical model including the voltage supply noise ratio to derive the resulting injection currents. This model allows determining the appropriate HFI voltage level for a given $\mathrm{SNR_{dB}}$ and a required maximum position error. The overall improvement is a reduction of the resulting injection currents that lead to a better efficiency and a lower rate of torque ripples. The HFI scheme becomes more attractive for sensorless application or as a redundant position sensor in a fault tolerant strategy.

REFERENCES

[1] S. M. Widyan and R. E. Hanitsch, "High-power density radial-flux permanent-magnet sinusoidal three-phase three-slot four-pole electrical generator," *Int. J. Elect. Power Energy Syst.*, vol. 43, pp. 1221–1227, 2012.

[2] Q. Gao, S. Shen, and T. Wang, "A novel drive strategy for PMSM compressor," in *Proc. Int. Conf. Elect. Control Eng.*, Jun. 2010, pp. 3192–3195.

[3] S. Yu, Z. Yang, S. Wang, and K. Zheng, "Sensorless adaptive backstepping speed tracking control of uncertain permanent magnet synchronous motors," in *Proc. IEEE Int. Symp. Circuits Syst.*, Jun. 2010, pp. 1131–1135.

[4] Z. Peroutka, K. Zeman, F. Krus, and F. Kosten, "New generation of trams with gearless wheel PMSM drives: From simple diagnostics to sensorless control," in *Proc. 14th Int. Power Electron. Motion Control Conf.*, Sep. 2010, pp. 31–36.

[5] J. Holtz, "Sensorless control of induction machines—with or without signal injection?" *IEEE Trans. Ind. Electron.*, vol. 53, no. 1, pp. 7–30, Feb. 2006.

[6] P. P. Acarnley and J. F. Watson, "Review of position-sensorless operation of brushless permanent-magnet machines," *IEEE Trans. Ind. Electron.*, vol. 53, no. 2, pp. 352–362, Apr. 2006.

[7] M. Pacas, "Sensorless drives in industrial applications," *IEEE Ind. Electron. Mag.*, vol. 5, no. 2, pp. 16–23, Jun. 2011.

[8] F. Zidani, D. Diallo, and M. E. H. Benbouzid, "A fuzzy-based approach for the diagnosis of fault modes in a voltage-fed PWM inverter induction motor drive," *IEEE Trans. Ind. Electron.*, vol. 55, no 2, pp. 586–593, Feb. 2008.

[9] F-J. Lin, Y.-C., J.-M. Chen, and C.-M. Yeh, "Sensorless IPMSM drive system using saliency back-EMF-based intelligent torque observer with MTPA control," *IEEE Trans. Ind. Informat.*, vol. 10, no. 2, pp. 1226–1241, May 2014.

[10] J. Holland, *Adaptation in Natural and Artificial Systems*. Cambridge, MA, USA: MIT Press, 1975.

[11] Y. Liang and Y. Li, "Sensorless control of PM synchronous motors based on MRAS method and initial position estimation," in *Proc. 6th Int. Conf. Elect. Mach. Syst.*, Nov. 9–11, 2003, vol. 1, pp. 96–99.

[12] S. Bolognani, L. Tubiana, and M. Zigliotto, "EKF-based sensorless IPM synchronous motor drive for flux-weakening applications," *IEEE Trans. Ind. Appl.*, vol. 39, no. 3, pp. 768–775, May/Jun. 2003.

[13] Li. Changsheng and M. Melbuluk, "A sliding mode observer for sensorless control of permanent magnet synchronous motors," in *Proc. 36th Annu. Meeting Conf. Rec. Ind. Appl.*, Sep./Oct. 2001, vol. 2, pp. 1273–1278.

[14] A. Arias, O. Carlos, Z. Jordi, J. Espina, and J. Pou," Hybrid sensorless permanent magnet synchronous machine four quadrant drive based on direct matrix converter," *Elect. Power Energy Syst.*, vol. 45, pp. 78–86, 2013.

[15] P. L. Jansen and R. D. Lorenz," Transducerless position and velocity estimation in induction and salient AC machines," *IEEE Trans. Ind. Appl.*, vol. 31, no. 2, pp. 240–247, Mar./Apr. 1995.

[16] J. Cilia, G. M. Asher, K. J. Bradley, and M. Sumner, "Sensorless position detection for vector-controlled induction motor drives using an asymmetric outer-section cage," *IEEE Trans. Ind. Appl.*, vol. 33, no. 5, pp. 1162–1169, Sep./Oct. 1997.

[17] N. Teske, G. M. Asher, M. Sumner, and K. J. Bradley, "Encoderless position estimation for symmetric cage induction machines under loaded conditions," *IEEE Trans. Ind. Appl.*, vol. 37, no. 6, pp. 1793–1800, Nov./Dec. 2001.

[18] O. Mansouri-Toudert, H. Zeroug, F. Auger, and A. Chibah, "Improved rotor position estimation of salient-pole PMSM using high frequency carrier signal injection," in *Proc. IEEE Int. Conf. Mechatronics*, Vicenza, Italy, Feb. 27–Mar. 1, 2013, pp. 761–767.

[19] A. Arias, C. Silva, G. M. Asher, J. C. Clare, and P. W. Wheeler, "Use of a matrix converter to enhance the sensorless control of a surface-mount permanent-magnet AC motor at zero and low frequency," *IEEE Trans. Electron.*, vol. 53, no. 2, pp. 440–449, Apr. 2006.

[20] S. Damkhi, M. S. Nait Said, and N. Nait Said, "Slotting effects and high frequency signal injection for induction machine rotor speed estimation," in *Proc. Int. Conf. Expo. Elect. Power Eng.*, Iasi, Romania, Oct. 25–27, 2012, pp. 401–408.

[21] C. Silva, G. M. Asher, and M. Sumner, "Hybrid rotor position observer for wide speed-range sensorless PM motor drives including zero speed," *IEEE Trans. Ind. Electron.*, vol. 53, no. 2, pp. 373–378, Apr. 2006

[22] M. W. Degner and R. D. Lorenz, "Using multiple saliencies of the estimation of flux, position, and velocity in AC machines," *IEEE Trans. Ind. Appl.*, vol. 34, no. 5, pp. 1097–1104, Sep./Oct. 1998.

[23] P. Yongsoon and S. Seung-Ki, "A novel method utilizing trapezoidal voltage to compensate for inverter nonlinearity," *IEEE Trans. Power Electron.*, vol. 27, no. 12, pp. 4837–4846, Dec. 2012.

[24] P. Yongsoon and S. Seung-Ki, "Implementation schemes to compensate for inverter nonlinearity based on trapezoidal voltage," *IEEE Trans. Ind. Appl.*, vol. 50, no. 2, pp. 1066–1073, Mar./Apr. 2014.

[25] P. Yongsoon and S. Seung-Ki, "Sensorless control method for PMSM based on frequency-adaptive disturbance observer," *IEEE J. Emerg. Sel. Topics Power Electron.*, vol. 2, no. 2, pp. 143–151, Jun. 2014.

Slimane Medjmadj received the Eng. and Magister degrees in electrotechnique from the University of Ferhat Abbas Setif, Setif, Algeria, in 1996 and 2005, respectively. He is currently working toward the Ph.D. degree at the University of Setif, Setif.

He is an Assistant Professor in the Department of Electromecanique, Mohammed El Bachir El Ibrahimi University, Bordj Bou Arréridj, Algeria. He is a Member of the Laboratory of Control (LAS), University of Setif. His main research interests include diagnosis and fault tolerant control of electric drives.

Demba Diallo (SM'05) received the M.Sc. and Ph.D. degrees in electrical and computer engineering from the National Polytechnic Institute of Grenoble, Grenoble, France, in 1990 and 1993, respectively.

He is currently working with the Laboratoire de Génie Electrique de Paris, Paris, France. He is the Head of the Design, Control, and Diagnosis Team. His area of research interests include advanced control techniques and diagnosis of ac drives, design of electric powertrains, and autonomous systems.

Dr. Diallo is an Editor of the IEEE TRANSACTIONS ON VEHICULAR TECHNOLOGY.

Mohammed Mostefai was born in Bordj Bou Arreridj, Algeria, in April 1965. He received the M.Sc. degree in electrical engineering from the University of Setif, Setif, Algeria, in 1988, and the Ph.D. degree in control and software engineering from the University of Lille, Villeneuve d'Ascq, France, in 1994.

He is currently a Full Professor at the University of Setif. He has held several scientific and administrative responsibilities since February 2006, first as a President of the Scientific Committee, then as a Director of the Laboratory of Control (LAS), and finally, as the Vice President for Research at the University of Setif. His research interests include study, modeling, analysis, and control of industrial systems. The mainly covered applications are production systems ranging from electro-energy systems (electric machines and networks) to large automated manufacturing systems.

Claude Delpha (M'08) received the Ph.D. degree in signal processing for smart systems from the University of Metz, France.

Since 2001, he has been with the Laboratoire des Signaux et Systèmes, Gif Sur Yvette, France. He is currently an Associate Professor at the University Paris-Sud, Orsay, France. He works in the field of signal processing for security and system monitoring (multimedia and smart systems). His main areas of research interests include multidimensional signal processing, data hiding (watermarking, steganography), pattern recognition, fault detection, and diagnosis (incipient and intermittent).

Antoni Arias (M'03) received the B.Eng. degree in electrical engineering, and the M.Eng. and Ph.D. degrees in control and electronic engineering from the Universitat Politècnica de Catalunya (UPC), Catalonia, Spain, in 1993, 1997, and 2001 respectively.

From 1992 to 1995, he was with SADECT, Barcelona, Spain, a local industrial electronics company. Since 1996, he has been a Lecturer at UPC, where he was appointed as an Associate Professor in 2002. In 1999, he was a Visiting Research Assistant and part time Lecturer at the University of Glamorgan, Pontypridd, Wales, U.K. In 2003 and 2004, he joined as a Visiting Fellow at the Power Electronics, Machines, and Control Group, University of Nottingham, Nottingham, U.K. In 2011 and 2012, he was with the Laboratoire de Génie Electrique de Paris, Paris, France, as an Invited Associate Professor. His research interests include sensorless variable-speed drive systems, power electronics converters, and control strategies.